

Copyright © 1995, by the author(s).
All rights reserved.

Permission to make digital or hard copies of all or part of this work for personal or classroom use is granted without fee provided that copies are not made or distributed for profit or commercial advantage and that copies bear this notice and the full citation on the first page. To copy otherwise, to republish, to post on servers or to redistribute to lists, requires prior specific permission.

**SYNCHRONIZATION OF CHUA'S CIRCUITS WITH
TIME-VARYING CHANNELS AND PARAMETERS**

by

Leon O. Chua, Tao Yang, Guo-Qun Zhong, and Chai Wah Wu

Memorandum No. UCB/ERL M95/76

1 June 1995

**SYNCHRONIZATION OF CHUA'S CIRCUITS WITH
TIME-VARYING CHANNELS AND PARAMETERS**

by

Leon O. Chua, Tao Yang, Guo-Qun Zhong, and Chai Wah Wu

Memorandum No. UCB/ERL M95/76

1 June 1995

ELECTRONICS RESEARCH LABORATORY

**College of Engineering
University of California, Berkeley
94720**

Synchronization of Chua's Circuits with Time-varying Channels and Parameters

Leon O. Chua, Tao Yang*, Guo-Qun Zhong[†] and Chai Wah Wu
Electronics Research Laboratory and
Department of Electrical Engineering and Computer Sciences,
University of California at Berkeley,
Berkeley, CA 94720, U.S.A.

*Visiting scholar on leave from the Department of Automatic Control Engineering, Shanghai University of Technology, 149 Yan Chang Road, Shanghai 200072, P.R.China.

[†]Visiting scholar on leave from Guangzhou Institute of Electronic Technology, Academia Sinica, Guangzhou 510070, P.R.China.

Abstract

In this paper, we study the use of adaptive controllers to maintain the synchronization of two Chua's circuits with time-varying channel and time-varying parameters. Both simulation results and experimental results are provided to verify the operation of the designs.

1 Introduction

Because of its potential applications to spread spectrum communication, the synchronization of chaotic systems has been studied extensively both in theory and in experiments[1—17]. However, in almost all the previous work, the driving and the driven chaotic systems are supposed to be identical and their parameters are supposed to be time-invariant. The channel through which the transmitted signal is transmitted is also supposed to be time-invariant. The above assumptions limit its applicability in practical solutions.

So far, all chaos-based communication systems use chaotic systems both as transmitters and receivers. The transmitter generates a chaotic signal which is used to encode the message signal in different ways, for example: chaotic masking[1—3], parameter modulation[8,9] and state variable modulation[5,6,17]. Chaotic masking is not very secure if the message is directly added onto the chaotic masking signal. The authors of [4] and [19] demonstrated that the smaller the message signal is, the lower the degree of security will be. Chaotic switching is the easiest form of parameter modulation and it was also shown to have a low degree of security[20] if the parameters of the transmitter are not chosen carefully. State variable modulation uses a functional of the message signal to modulate the state variables of the transmitter and hides the message signal, which is usually a narrow band signal, into the broad band chaotic signal.

The transmitted signal is then transmitted to the receiver, which is an identical chaotic system. The transmitted signal will synchronize the receiver to the transmitter to obtain a replica of the chaotic masking signal.

Most of the methods presented so far require that the parameters of the transmitter and the receiver are identical, and the channel is time-invariant. It has been shown that a time-varying channel can desynchronize the system.

In this paper, we use adaptive controllers to maintain the synchronization between the transmitter and the receiver when the parameters of the transmitter are time-varying or the channel is memoryless and time-varying. We used Chua's circuits as our driving and driven system. The feedback into the adaptive controller is the synchronization error, which measures the degree of de-synchronization

between the transmitter and receiver.

The organization of this paper is as follows. In section 2, adaptive controllers are presented which compensate the time-varying channel gain. In section 3, adaptive controllers are presented which compensate the time-varying parameters. In section 4, experimental results are presented.

2 Adaptive controllers for time-varying channel compensation

In this paper, all the results are based on Chua's circuit[18,21], which exhibits a family of chaotic attractors and can be easily implemented in hardware. As shown in Fig.1(a), Chua's circuit consists of a linear inductor L , a linear resistor R , two linear capacitors C_1 and C_2 and a nonlinear resistor—the Chua's diode N_R . The state equations for Chua's circuit are given by:

$$\begin{cases} \frac{dv_1}{dt} = \frac{1}{C_1}[G(v_2 - v_1) - f(v_1)] \\ \frac{dv_2}{dt} = \frac{1}{C_2}[G(v_1 - v_2) + i_3] \\ \frac{di_3}{dt} = \frac{1}{L}[-v_2 - R_0 i_3] \end{cases} \quad (1)$$

where v_1, v_2 and i_3 are the voltage across C_1 , the voltage across C_2 and the current through L , respectively. We set $G = \frac{1}{R}$. The term $R_0 i_3$ is added to account for the small resistance of the inductor in the physical circuit. $f(v_1)$, the piece-wise linear $v - i$ characteristic of the Chua's diode, is given by:

$$f(v_1) = G_b v_1 + \frac{1}{2}(G_a - G_b)(|v_1 + E| - |v_1 - E|) \quad (2)$$

where E is the breakpoint voltage of the Chua's diode as shown in Fig.1(b).

We use the synchronization scheme shown in Fig.2[12]. The state equations are given by:

$$\begin{cases} \frac{dv_1}{dt} = \frac{1}{C_1}[G(v_2 - v_1) - f(v_1)] \\ \frac{dv_2}{dt} = \frac{1}{C_2}[G(v_1 - v_2) + i_3] \\ \frac{di_3}{dt} = \frac{1}{L}[-v_2 - R_0 i_3] \end{cases} \quad (3)$$

$$\begin{cases} \frac{d\tilde{v}_1}{dt} = \frac{1}{C_1}[G(\tilde{v}_2 - \tilde{v}_1) - f(\tilde{v}_1) + K_1(s(t) - \tilde{v}_1)] \\ \frac{d\tilde{v}_2}{dt} = \frac{1}{C_2}[G(\tilde{v}_1 - \tilde{v}_2) + \tilde{i}_3] \\ \frac{d\tilde{i}_3}{dt} = \frac{1}{L}[-\tilde{v}_2 - R_0 \tilde{i}_3] \end{cases} \quad (4)$$

where $s(t) = K_c(t)v_1$, and $K_c(t)$ is the time varying gain of the channel. Constant unity gain channel corresponds to $K_c(t) = 1$.

In this section we study how to compensate for the time-varying channel gain $K_c(t)$. In the driven system, we construct an adaptive gain $K_r(t)$ such that $K_c(t)K_r(t) \rightarrow 1$ as $t \rightarrow \infty$ to maintain the synchronization. Then the driven system should be rewritten as:

$$\begin{cases} \frac{d\tilde{v}_1}{dt} = \frac{1}{C_1}[G(\tilde{v}_2 - \tilde{v}_1) - f(\tilde{v}_1) + K_1(K_r(t)s(t) - \tilde{v}_1)] \\ \frac{d\tilde{v}_2}{dt} = \frac{1}{C_2}[G(\tilde{v}_1 - \tilde{v}_2) + \tilde{i}_3] \\ \frac{d\tilde{i}_3}{dt} = \frac{1}{L}[-\tilde{v}_2 - R_0\tilde{i}_3] \end{cases} \quad (5)$$

The dynamics of $K_r(t)$ is given by one of the following adaptive controllers:

Controller #1

$$\dot{K}_r(t) = -k_1(K_r(t)|s(t)| - |\tilde{v}_1|) \quad (6)$$

Controller #2

$$\dot{K}_r(t) = -k_1(K_r(t)s^2(t) - s(t)\tilde{v}_1) \quad (7)$$

Controller #3

$$\begin{aligned} \dot{K}_r(t) &= -k_1 \operatorname{sgn}\left(\frac{\partial \tilde{v}_1}{\partial K_r}\right)(K_r(t)s(t) - \tilde{v}_1) \\ &= -k_1 \operatorname{sgn}(K_1 s(t))(K_r(t)s(t) - \tilde{v}_1) \end{aligned} \quad (8)$$

In our simulations, the parameters of Chua's circuit are given by: $C_1 = 5.56nF$, $C_2 = 50nF$, $G = 0.70028$, $L = 7.14mH$, $R_0 = 0\Omega$, $G_a = -0.8mS$, $G_b = -0.5mS$, $E = 1v$. $K_1 = 0.01$. The Chua's circuit exhibits a double scroll Chua's attractor for these parameters. We choose the synchronization error to be $v_1 - \tilde{v}_1$. In all of our simulations, the initial conditions of the transmitter and the receiver are $(v_1(0), v_2(0), i_3(0)) = (-0.2V, -0.02V, 0.1mA)$ and $(\tilde{v}_1(0), \tilde{v}_2(0), \tilde{i}_3(0)) = (0.02V, -0.12V, -0.1mA)$, respectively. So the transmitter and the receiver are initially desynchronized. The fourth order Runge-Kutta method with fixed step-size $h = 10^{-6}s$ is used to simulate the system.

Fig.3 shows the simulation results when $K_c(t)$ is a sinusoidal function as follows:

$$K_c(t) = 0.5 - 0.1\sin(75\pi t) \quad (9)$$

and controller #1 is used with $k_1 = 10^6$.

Fig.3(a) shows $K_c(t), K_r(t)$ and $K_c(t)K_r(t)$. We can see that $K_r(t)$ asymptotically approaches $\frac{1}{K_c(t)}$, and the settling time is about $0.6ms$. Fig.3(b) shows the synchronization error $v_1(t) - \bar{v}_1(t)$. For comparison, the synchronization error in the case when no adaptive controller is used is shown in Fig.3(c). One can see that the synchronization error is reduced significantly by using the adaptive controller.

Fig.4 shows the simulation results when $K_c(t)$ is a sinusoidal function as shown in Eq.(9) and controller #2 is used with $k_1 = 10^6$. Fig.4(a) shows $K_c(t), K_r(t)$ and $K_c(t)K_r(t)$. We can see that $K_r(t)$ asymptotically approaches $\frac{1}{K_c(t)}$, and the settling time is about $0.6ms$. Fig.4(b) shows the synchronization error $v_1(t) - \bar{v}_1(t)$, which is also reduced significantly compared with that shown in Fig.3(c).

Fig.5 shows the simulation results when $K_c(t)$ is a sinusoidal function as shown in Eq.(9) and controller #3 is used with $k_1 = 10^6$. Fig.5(a) shows $K_c(t), K_r(t)$ and $K_c(t)K_r(t)$. We can see that the settling time is about $0.6ms$. Fig.5(b) shows the synchronization error $v_1(t) - \bar{v}_1(t)$.

When the coupling factor K_1 becomes too small, the transmitter and the receiver will be desynchronized even when the channel has a unit gain $K_c(t) = 1$ for all time. Fig. 6(a) shows this de-synchronization with $K_1 = 0.0005$. However, we find that the adaptive controllers used can also compensate for this kind of de-synchronization. Fig.6(b) shows the simulation result when $K_c(t) = 1$ and $K_1 = 0.0005$, and controller #1 with $k_1 = 10^6$ is used. We see that the synchronization error approaches 0.

3 Adaptive controller for time-varying parameter compensation

Parameter mismatch can also result in the loss of synchronization of the system shown in Fig.2. Although the synchronization is robust in the sense that it can tolerate some parameter mismatch[10], the authors of [5] gave an experimental example showing that a 1% resistor mismatch can sharply reduce the quality of the received signal.

In this section, we study the synchronization in the cases where the parameters of the transmitter

are time-varying. In this case, we rewrite the driving system as follows:

$$\begin{cases} \frac{dv_1}{dt} = \frac{K_{C_1}(t)}{C_1} [K_G(t)G(v_2 - v_1) - f(v_1)] \\ \frac{dv_2}{dt} = \frac{K_{C_2}(t)}{C_2} [K_G(t)G(v_1 - v_2) + i_3] \\ \frac{di_3}{dt} = \frac{K_L(t)}{L} [-v_2 - (K_{R_0}(t) + R_0)i_3] \end{cases} \quad (10)$$

where $K_{C_1}(t)$, $K_{C_2}(t)$, $K_L(t)$, $K_{R_0}(t)$ and $K_G(t)$ are the time-varying factors of the parameters C_1, C_2, L, R_0 and G , respectively.

The driven system is as follows:

$$\begin{cases} \frac{d\tilde{v}_1}{dt} = \frac{\tilde{K}_{C_1}(t)}{C_1} [\tilde{K}_G(t)G(\tilde{v}_2 - \tilde{v}_1) - f(\tilde{v}_1) + K_1(v_1 - \tilde{v}_1)] \\ \frac{d\tilde{v}_2}{dt} = \frac{\tilde{K}_{C_2}(t)}{C_2} [\tilde{K}_G(t)G(\tilde{v}_1 - \tilde{v}_2) + \tilde{i}_3 + K_1(v_1 - \tilde{v}_1)] \\ \frac{d\tilde{i}_3}{dt} = \frac{\tilde{K}_L(t)}{L} [-\tilde{v}_2 - (\tilde{K}_{R_0}(t) + R_0)\tilde{i}_3 + K_1(v_1 - \tilde{v}_1)] \end{cases} \quad (11)$$

where $\tilde{K}_{C_1}(t)$, $\tilde{K}_{C_2}(t)$, $\tilde{K}_L(t)$, $\tilde{K}_{R_0}(t)$ and $\tilde{K}_G(t)$ are compensating adjustments of the parameters C_1, C_2, L, R_0 and G , respectively, which are adaptively modified by using the following adaptive controllers. In this paper, we consider the cases when only one parameter is time-varying at a time.

1. Compensating for K_G

The controller is chosen as:

$$\begin{aligned} \dot{\tilde{K}}_G(t) &= k_1 \operatorname{sgn}\left(\frac{\partial \tilde{v}_1}{\partial \tilde{K}_G}\right)(v_1 - \tilde{v}_1) \\ &= k_1 \operatorname{sgn}\left(\frac{1}{C_1} G(\tilde{v}_2 - \tilde{v}_1)\right)(v_1 - \tilde{v}_1) \end{aligned} \quad (12)$$

The simulation results are shown in Fig.7 with $k_1 = 10^6$. $K_G(t)$ is a sinusoidal function as follows:

$$1.1 - 0.05 \sin\left(\frac{15\pi}{2}t\right) \quad (13)$$

Fig.7(a) shows $K_G(t)$ (dashed line) and $\tilde{K}_G(t)$ (solid line). One can see that $\tilde{K}_G(t)$ asymptotically approaches $K_G(t)$ with a settling time of about 3ms. Fig.7(b) shows the synchronization error. Note in Fig.7(a) that from 45.5ms to 63ms, $\tilde{K}_G(t)$ is almost constant while $K_G(t)$ decreases. This is because in the parameter range corresponding to the waveform of $K_G(t)$ during 45.5ms to 63ms, the synchronization is maintained even though $\tilde{K}_G(t) \neq K_G(t)$. In Fig.7(c) we show the synchronization error without the adaptive controller and we can see that in the period 45.5ms to 63ms the synchronization error is small.

2. Compensating for K_{C_1}

In this case, the controller used is:

$$\begin{aligned}\dot{\tilde{K}}_{C_1}(t) &= k_1 \text{sgn}\left(\frac{\partial \dot{\tilde{v}}_1}{\partial \tilde{K}_{C_1}}\right)(v_1 - \tilde{v}_1) \\ &= k_1 \text{sgn}\left(\frac{1}{C_1}[G(\tilde{v}_2 - \tilde{v}_1) - f(\tilde{v}_1) + K_1(v_1 - \tilde{v}_1)]\right)(v_1 - \tilde{v}_1)\end{aligned}\quad (14)$$

The simulation results are shown in Fig.8 with $k_1 = 2 \times 10^6$. $K_{C_1}(t)$ is a sinusoidal function shown in Eq.(13). From Fig.8(a) one can see that $\tilde{K}_{C_1}(t)$ asymptotically approaches $K_{C_1}(t)$ with a settling time of about 1ms. Fig.8(b) shows the synchronization error.

3. Compensating for K_{C_2}

In this case, the controller is:

$$\begin{aligned}\dot{\tilde{K}}_{C_2}(t) &= k_1 \text{sgn}\left(\frac{\partial \dot{\tilde{v}}_2}{\partial \tilde{K}_{C_2}}\right)(v_1 - \tilde{v}_1) \\ &= k_1 \text{sgn}\left(\frac{1}{C_2}[G(\tilde{v}_1 - \tilde{v}_2) + \tilde{i}_3 + K_1(v_1 - \tilde{v}_1)]\right)(v_1 - \tilde{v}_1)\end{aligned}\quad (15)$$

The simulation results are shown in Fig.9 with $k_1 = 10^6$. $K_{C_2}(t)$ is a sinusoidal function shown in Eq.(13). Fig.9(a) shows $K_{C_2}(t)$ and $\tilde{K}_{C_2}(t)$. One can see that $\tilde{K}_{C_2}(t)$ approaches $K_{C_2}(t)$ asymptotically with a settling time of about 2ms. Fig.9(b) shows the synchronization error.

4. Compensating for K_L

In this case, the controller is:

$$\begin{aligned}\dot{\tilde{K}}_L(t) &= k_1 \text{sgn}\left(\frac{\partial \dot{\tilde{i}}_3}{\partial \tilde{K}_L}\right)(v_1(t) - \tilde{v}_1) \\ &= k_1 \text{sgn}\left(\frac{1}{L}[-\tilde{v}_2 - R_0 \tilde{i}_3 + K_1(v_1 - \tilde{v}_1)]\right)(v_1 - \tilde{v}_1)\end{aligned}\quad (16)$$

The simulation results are shown in Fig.10 with $k_1 = 10^6$. $K_L(t)$ is a sinusoidal function shown in Eq.(13). Fig.10(a) shows $K_L(t)$ and $\tilde{K}_L(t)$. One can see that the settling time is about 2ms. Fig.10(b) shows the synchronization error.

5. Compensating for K_{R_0}

In this case, the controller is:

$$\dot{\tilde{K}}_{R_0}(t) = k_1 \text{sgn}\left(\frac{\partial \dot{\tilde{i}}_3}{\partial \tilde{K}_{R_0}}\right)(v_1(t) - \tilde{v}_1)\quad (17)$$

$$= k_1 \text{sgn}\left(-\frac{\dot{i}_3}{L}\right)(v_1 - \tilde{v}_1)$$

The simulation results are shown in Fig.11 with $k_1 = 10^8$. $K_{R_0}(t)$ is a sinusoidal function shown in Eq.(13). Fig.11(a) shows $K_{R_0}(t)$ and $\tilde{K}_{R_0}(t)$. One can see that $\tilde{K}_{R_0}(t)$ approaches $K_{R_0}(t)$ with a settling time of about 1.5ms. Fig.11(b) shows the synchronization error.

4 Experimental results

In this section we supplement the computer simulation results with experimental results from a physical circuit implementation. The circuit diagram of the system used to study the synchronization between two Chua's circuits when the channel is time-varying is shown in Fig.12. In our experiments, both Chua's circuits are identical and have the following parameters: $C_1 = 6.8nF$, $C_2 = 68nF$, $L = 18.4mH$, $R_0 = 12\Omega$, $R = 1.98k\Omega$, $G_a = -0.73mS$, $G_b = -0.4mS$, $E = 1.8v$, $R_C = 3.8k\Omega$, where R_C is the coupling resistor, which satisfies $K_1 = \frac{1}{R_C}$.

The circuit parameters we used exhibits the Double Scroll Chua's attractor as shown in Fig.13. First , we show the synchronization between the transmitter and the receiver when the channel gain is 1. Fig.14(a) shows the relation between voltages $v_1(t)$ and $\tilde{v}_1(t)$, and Fig.14(b) shows the relation between voltages $v_2(t)$ and $\tilde{v}_2(t)$, where one can see that the transmitter and the receiver are synchronized.

When the channel gain drops to $K_c(t) = 0.65$, we find that the transmitter and the receiver are desynchronized. The relation between the voltages $v_1(t)$ and $\tilde{v}_1(t)$ is shown in Fig.15(a) and that between voltages $v_2(t)$ and $\tilde{v}_2(t)$ is shown in Fig.15(b).

Next we use the the adaptive controller as in Eq.(6), which is implemented using the circuit shown in Fig.12 to compensate for the channel gain which is set at $K_c(t) = 0.65$. The relation between voltages $v_1(t)$ and $\tilde{v}_1(t)$ is shown in Fig.16(a) and that between voltages $v_2(t)$ and $\tilde{v}_2(t)$ is shown in Fig.16(b). One can see that the synchronization is restored. Compare the results shown in Fig.16 with those shown in Fig.15, one can see that the effect of the adaptive controller is very significant.

Next, we study the effect of our controller under a weak coupling condition. In this case, the coupling resistor is $4.46k\Omega$, and as shown in Fig.17(a), this coupling without the aid of the controller is not big enough to synchronize the transmitter and the receiver even when a unity channel gain is used. Using the controller to compensate for this kind of de-synchronization we obtain the experimental result shown in Fig.17(b), where one can see that the synchronization is restored. In Fig.17(c), we

show the synchronization when the channel gain drops to 0.65 and the controller is used.

5 Conclusions

We have shown how two Chua's circuits can synchronize in the cases where the channel gain and the parameters are time-varying by using adaptive controllers in the receiver to compensate for the time-varying properties of the transmitter and the channel.

Although this paper is focused on the cases where only one parameter is time-varying and the others are kept constant, simulation results show that in the case of multiple time-varying parameters, the adaptive controllers can also perform good compensation to achieve synchronization.

Both simulation results and experimental results are presented for the proposed schemes. These results show that our methods can be useful for developing practical chaotic spread-spectrum communication systems.

References

- [1] L.Kocarev, K.S.Halle, K.Eckert, L.O.Chua and U.Parlitz, "Experimental demonstration of secure communications via chaotic synchronization," *Int. J. Bifurcation Chaos*, vol.2, no.3, pp.709-713, 1992.
- [2] K.M.Cuomo and A.V.Oppenheim, "Synchronization of Lorenz-based chaotic circuits with applications to communications," *IEEE Trans. Circuit Syst.*, vol.40, no.10, pp.626-633, Oct., 1993.
- [3] R.Lozi and L.O.Chua, "Secure communications via chaotic synchronization II: Noise reduction by cascading two identical receivers," *Int. J. Bifurcation Chaos*, vol.3, pp.1319-1325, 1993.
- [4] K.M.Short, "Steps toward unmasking secure communications," *Int. J. Bifurcation Chaos*, vol.4, pp.959-977, 1994.
- [5] K.S.Halle, C.W.Wu, M.Itoh and L.O.Chua, "Spread spectrum communication through modulation of chaos," *Int. J. Bifurcation Chaos*, vol.3, no.2, pp.469-477, 1993.
- [6] C.W.Wu and L.O.Chua, "A simple way to synchronize chaotic systems with applications to secure communication systems," *Int. J. Bifurcation Chaos*, vol.3, no.6, pp.1619-1627, 1993.
- [7] M.J.Ogorzalek, "Taming chaos—Part I: Synchronization," *IEEE Trans. Circuit Syst.-I*, vol.40, no.10, pp.693-699, Oct., 1993.
- [8] U.Parlitz, L.O.Chua, L.Kocarev, K.S.Halle and A.Shang, "Transmission of digital signal by chaotic synchronization," *Int. J. Bifurcation Chaos*, vol.2, no.4, pp.973-977, 1992.

- [9] T.L. Carroll, "Communicating with use of filtered, synchronized, chaotic signals," *IEEE Trans. Circuit Syst.-I*, vol.42, no.3, pp.105-110, Mar.1995.
- [10] C.W.Wu and L.O.Chua, "A unified framework for synchronization and control of dynamical systems," *Int. J. Bifurcation Chaos*, vol.4, no.4, pp.979-998, 1994.
- [11] C.W.Wu and L.O.Chua, "Synchronization in an array of linearly coupled dynamical systems," *IEEE Trans. Circuit and Syst.-I*, vol.42, no.8, pp.430-447, Aug. 1995.
- [12] L.O.Chua, K.Itoh, L.Kocarev and K.Eckert, "Chaos synchronization in Chua's circuit," *J. of circuit, systems and computers*, vol.3, no.1 pp.93-108, Mar. 1993.
- [13] P.Celka, "Synchronization of Chaotic systems through parameter adaptation," in *Proc. 1995 IEEE Int. Sym. on Circuits and systems*, pp.692-695, Seattle, Apr. 1995.
- [14] V.N.Belykh, N.N.Verichev, L.Kocarev and L.O.Chua, "On chaotic synchronization in a linear array of Chua's circuits," *J. of circuit, systems and computers*, vol.3, no.2, pp.579-589, 1993.
- [15] K.M.Cuomo, "Synthesizing self-synchronization chaotic arrays," *Int. J. Bifurcation Chaos*, vol.4, no.3, pp.727-736, 1994.
- [16] K.M.Cuomo, "Synthesizing self-synchronization chaotic systems," *Int. J. Bifurcation Chaos*, vol.3, no.5, pp.1327-1337, 1993.
- [17] C.W.Wu, G.Q.Zhong and L.O.Chua, "Synchronizing nonautonomous chaotic systems without phase-locking," to appear in *J. of circuit, systems and computers*.
- [18] J.M.Cruz and L.O.Chua, "An IC chip of Chua's circuit," *IEEE Trans. Circuit Syst.-II*, vol.40, no.10, pp.614-625, Oct.1993.
- [19] J.Stark and B.V.Arumugam, "Extracting slowly varying signals from a chaotic background," *Int. J. Bifurcation Chaos*, vol.2, pp.413-419, 1992.
- [20] T.Yang, "Recovery of digital signals from chaotic switching," to appear in *Int. J. Circuit Theory and Appls.*, 1995.
- [21] L.O.Chua, "Chua's circuit—An overview ten years later," *J. of circuit, systems and computers*, vol.4, no.2 pp.117-159, Jun. 1994.

Figure Caption

Figure 1 Chua's circuit and Chua's diode. (a) Chua's circuit, (b) Nonlinear v-i characteristic of Chua's diode.

Figure 2 The synchronization scheme of two Chua's circuits by using v_1 in a unidirectional driving configuration.

Figure 3. Synchronization of Chua's circuits when the channel gain $K_c(t)$ is a sinusoidal function and controller #1 is used. (a) The channel gain $K_c(t)$, gain of adaptive controller $K_r(t)$ and the product $K_c(t)K_r(t)$. (b) The synchronization error $(v_1 - \tilde{v}_1)$ when adaptive controller #1 is used. (c) The synchronization error $(v_1 - \tilde{v}_1)$ without using adaptive controller.

Figure 4. Synchronization of Chua's circuits when the channel gain $K_c(t)$ is a sinusoidal function and controller #2 is used. (a) The channel gain $K_c(t)$, gain of adaptive controller $K_r(t)$ and the product $K_c(t)K_r(t)$. (b) The synchronization error $(v_1 - \tilde{v}_1)$ when controller #2 is used.

Figure 5. Synchronization of Chua's circuits when the channel gain $K_c(t)$ is a sinusoidal function and controller #3 is used. (a) The channel gain $K_c(t)$, gain of adaptive controller $K_r(t)$ and the product $K_c(t)K_r(t)$. (b) The synchronization error $(v_1 - \tilde{v}_1)$ when controller #3 is used.

Figure 6(a) The synchronization error $(v_1 - \tilde{v}_1)$ when channel gain $K_c(t) = 1$ and a weak coupling factor $K_1 = 0.0005$ is used. No controller is used. (b) The synchronization error $(v_1 - \tilde{v}_1)$ when the channel gain $K_c(t)$ is 1 and a weak coupling factor $K_1 = 0.0005$ is used. Controller #1 is used.

Figure 7. Synchronization of Chua's circuits when G is a sinusoidal function of time. (a) $K_G(t)$ and $\tilde{K}_G(t)$. (b) The synchronization error $(v_1 - \tilde{v}_1)$ when the adaptive controller is used. (c) The synchronization error $(v_1 - \tilde{v}_1)$ without the adaptive controller.

Figure 8. Synchronization of Chua's circuits when C_1 is a sinusoidal function of time. (a) $K_{C_1}(t)$ and $\tilde{K}_{C_1}(t)$. (b) The synchronization error $(v_1 - \tilde{v}_1)$.

Figure 9. Synchronization of Chua's circuits when C_2 is a sinusoidal function of time. (a) $K_{C_2}(t)$ and $\tilde{K}_{C_2}(t)$. (b) The synchronization error $(v_1 - \tilde{v}_1)$.

Figure 10. Synchronization of Chua's circuits when L is a sinusoidal function of time. (a) $K_L(t)$ and $\tilde{K}_L(t)$. (b) The synchronization error $(v_1 - \tilde{v}_1)$.

Figure 11. Synchronization of Chua's circuits when R_0 is a sinusoidal function of time. (a) $K_{R_0}(t)$ and $\tilde{K}_{R_0}(t)$. (b) The synchronization error $(v_1 - \tilde{v}_1)$.

Figure 12 (a) Schematic diagram of the experimental circuit for studying the synchronization between two identical Chua's circuits under a time-varying channel. The equations of the adaptive

controller is given by Eq.(6). (b) Circuit with the absolute value transfer function.

Figure 13: The $v_1 - v_2$ phase portrait of the chaotic attractor in Chua's circuit used in the experiments.

Figure 14: With a unity channel gain, the transmitter and the receiver are synchronized with a $3.8k\Omega$ coupling resistor. (a) The relationship between v_1 and \tilde{v}_1 . (b) The relationship between v_2 and \tilde{v}_2 .

Figure 15: When the channel gain drops to 0.65, the transmitter and the receiver are desynchronized. No adaptive controller is used. (a) The relationship between v_1 and \tilde{v}_1 . (b) The relationship between v_2 and \tilde{v}_2 .

Figure 16: The adaptive controller in Fig.12 is used to compensate for the channel gain of 0.65. (a) The relationship between v_1 and \tilde{v}_1 . (b) The relationship between v_2 and \tilde{v}_2 .

Figure 17: The adaptive controller in Fig.12 can also compensate the de-synchronization caused by weak coupling. (a) The relationship between v_2 and \tilde{v}_2 shows the de-synchronization when the coupling resistor is $4.46k\Omega$ with a unity channel gain. No adaptive controller is used. (b) The relationship between v_2 and \tilde{v}_2 shows synchronization when the adaptive controller is used to compensate for the weak coupling factor with a unity channel gain. (c) The relationship between v_2 and \tilde{v}_2 shows synchronization when the adaptive controller is used to compensate for the weak coupling factor with a channel gain of 0.65.

Manuscript received _____

“Synchronization of Chua’s Circuits with Time-varying Channels and Parameters” by L. O. Chua, T. Yang, G-Q. Zhong and C. W. Wu.

Affiliation of authors

The authors are with the Electronics Research Laboratory and Department of Electrical Engineering and Computer Sciences, University of California at Berkeley, Berkeley, CA 94720.

T. Yang is on leave from the Department of Automatic Control Engineering, Shanghai University of Technology, 149 Yan Chang Road, Shanghai 200072, P. R. China.

G-Q. Zhong is on leave from Guangzhou Institute of Electronic Technology, Academia Sinica, Guangzhou 510070, P. R. China.

Acknowledgement of financial support

This work is supported in part by the Office of Naval Research under grant N00014-89-J-1402, by the National Science Foundation under grant MIP 86-14000, by the Josephine de Kármán Fellowship, and by the Joint Services Electronics Program under contract number F49620-94-C-0038. The United States Government is authorized to reproduce and distribute reprints for governmental purposes not withstanding any copyright notation hereon.

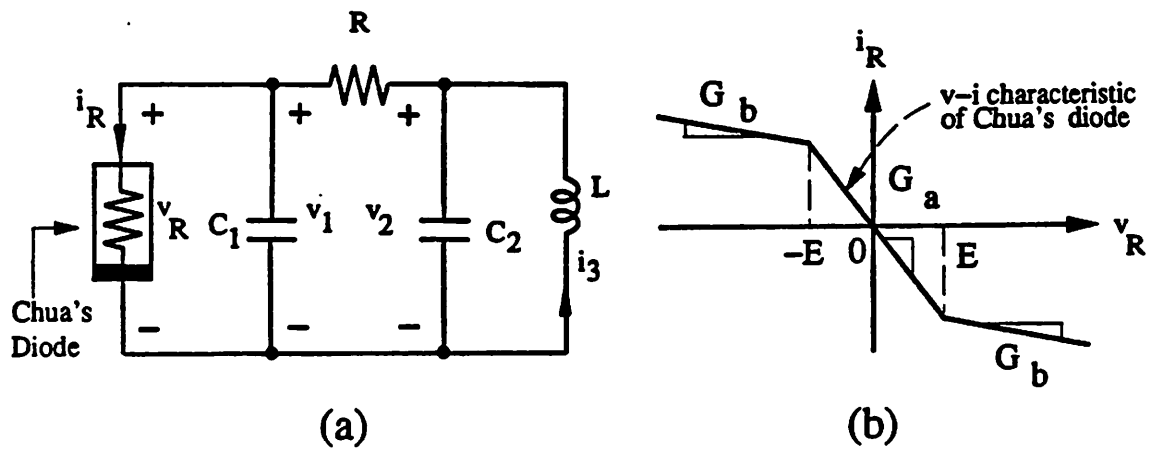


Figure 1

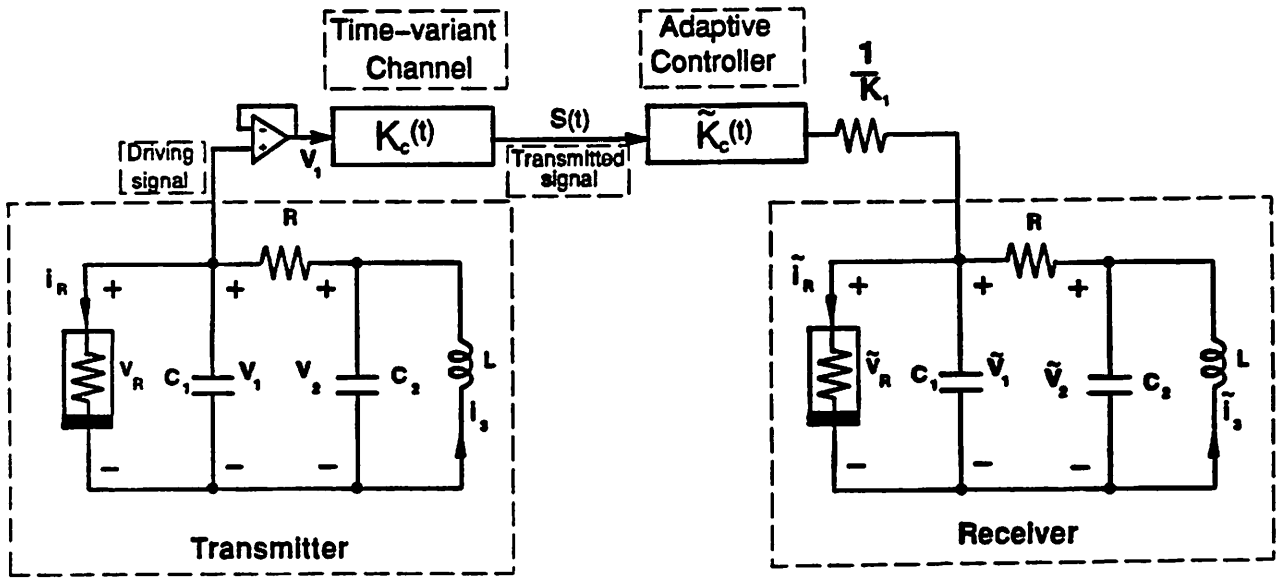


Figure 2

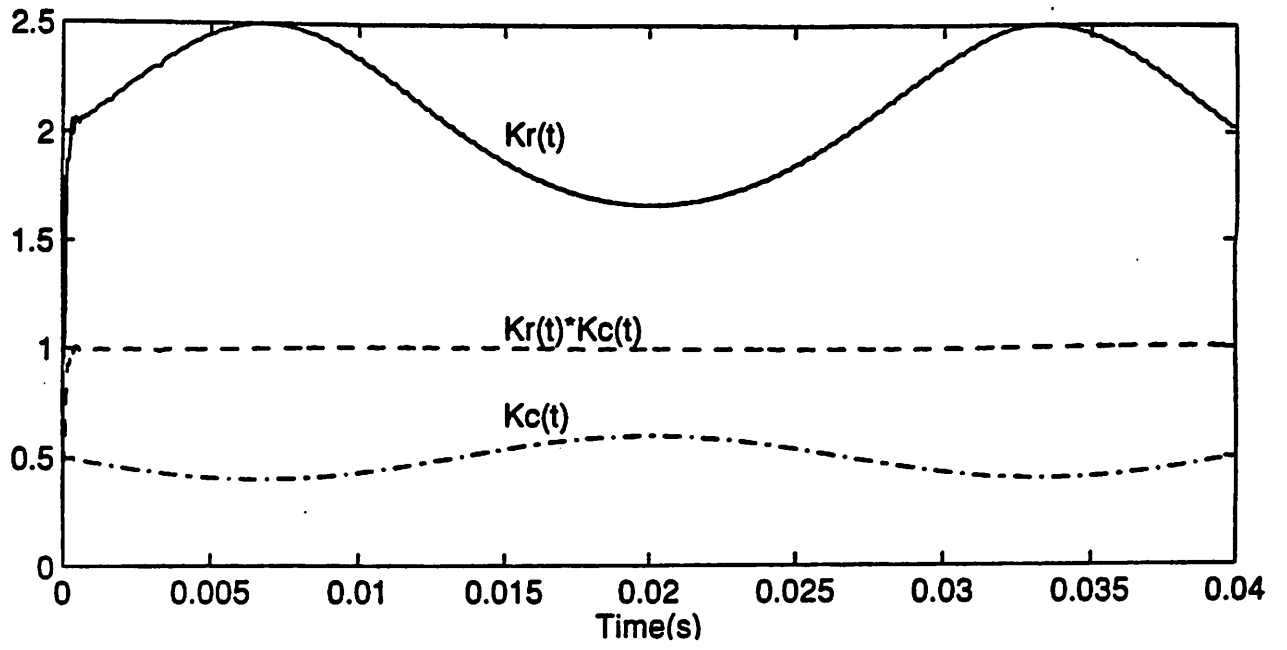


Figure 3(a)

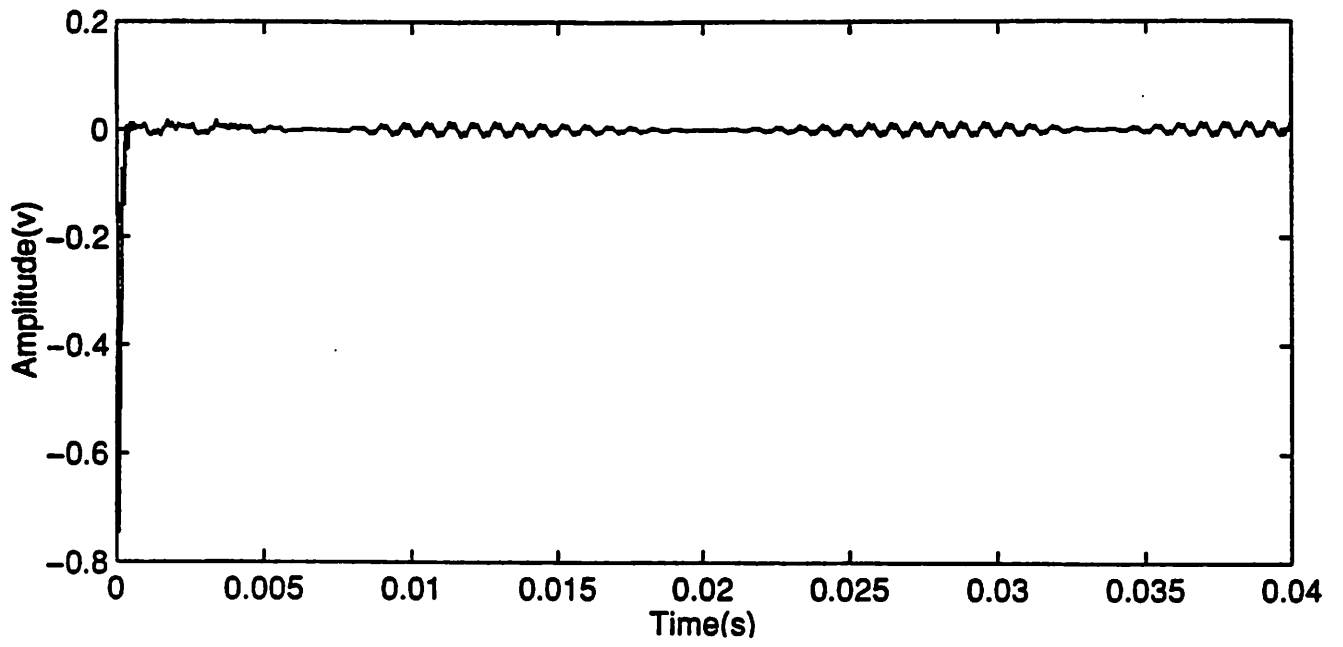


Figure 3(b)

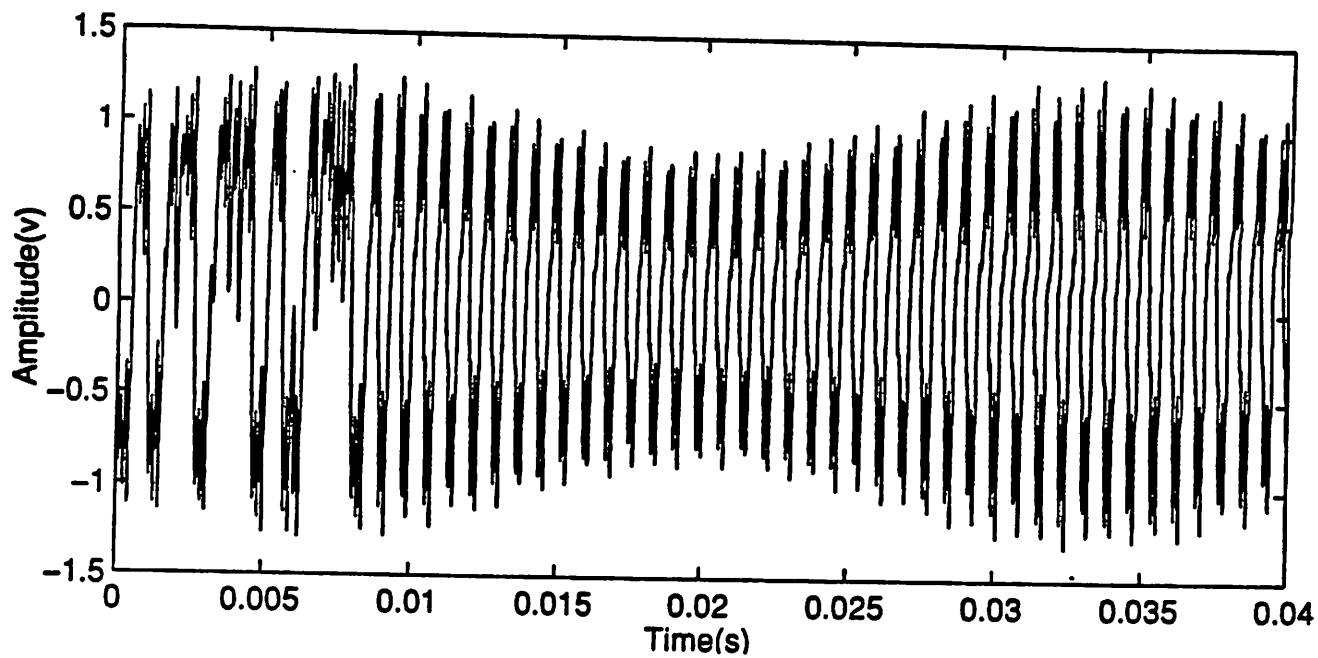


Figure 3(c)

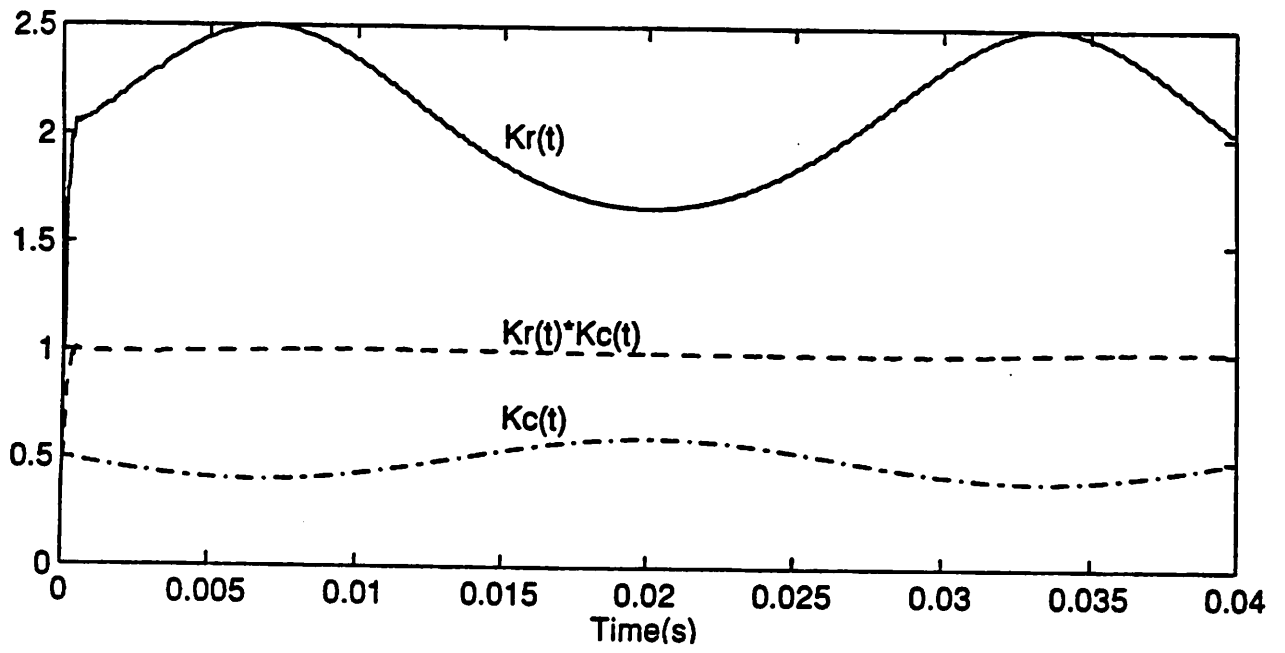


Figure 4(a)

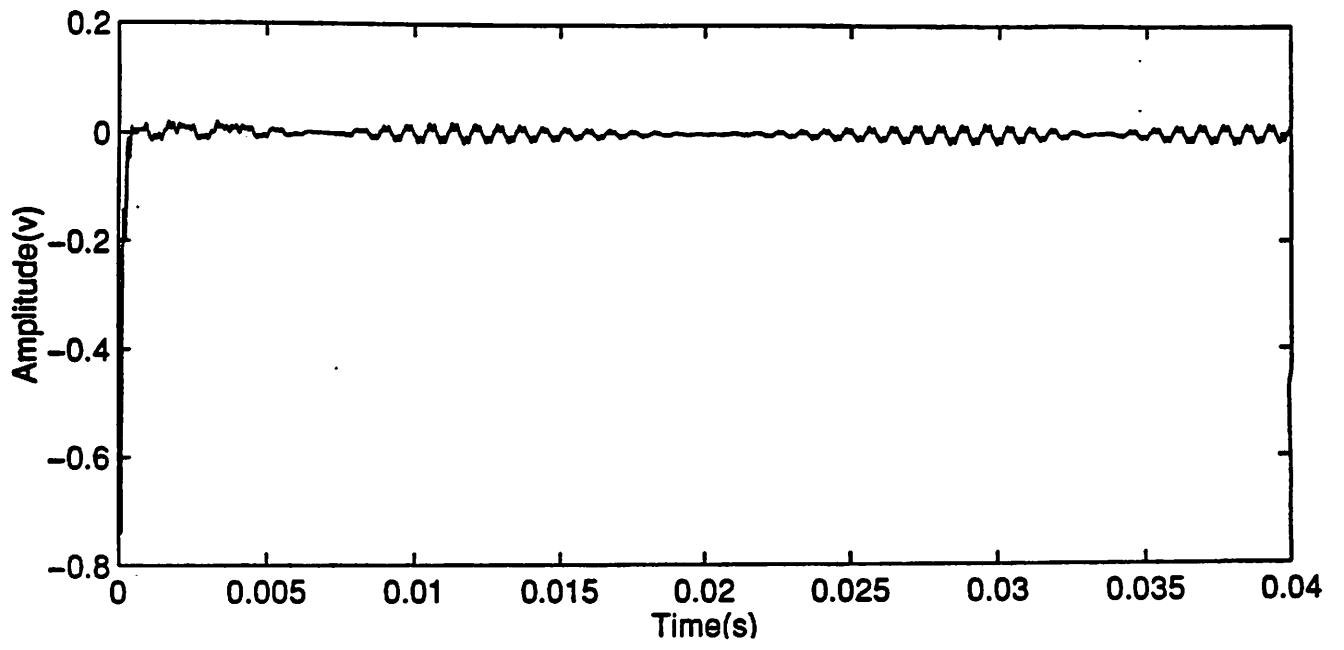


Figure 4(b)

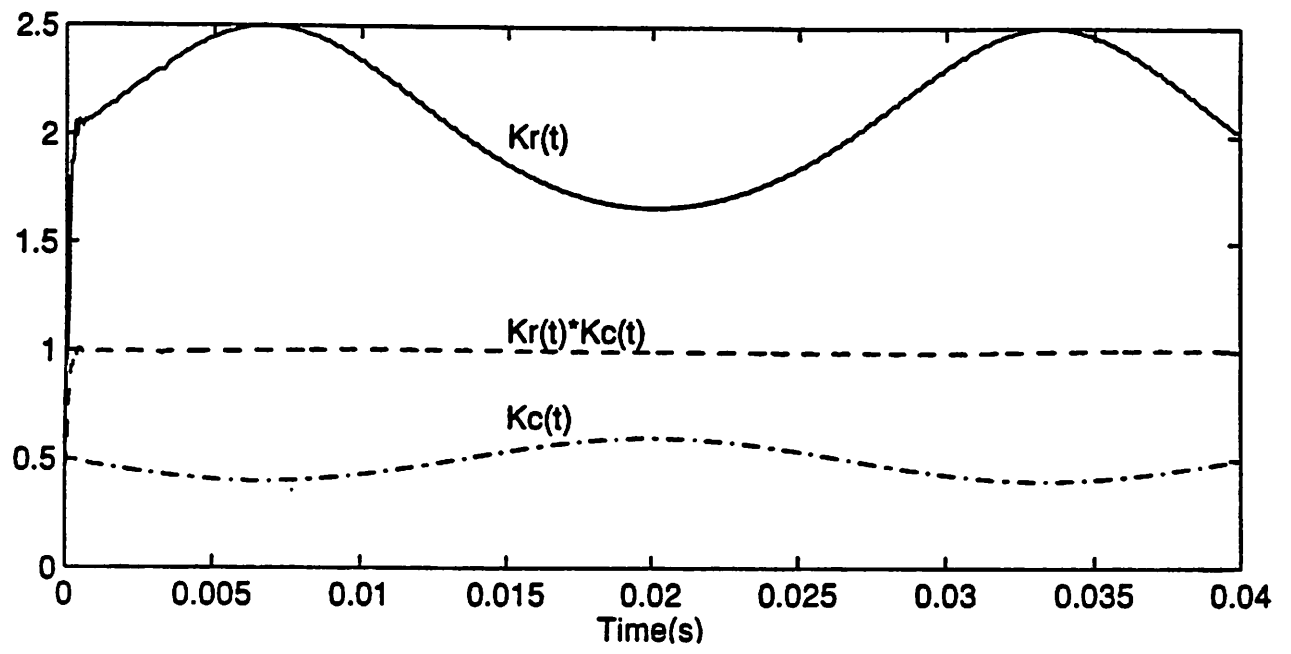


Figure 5(a)

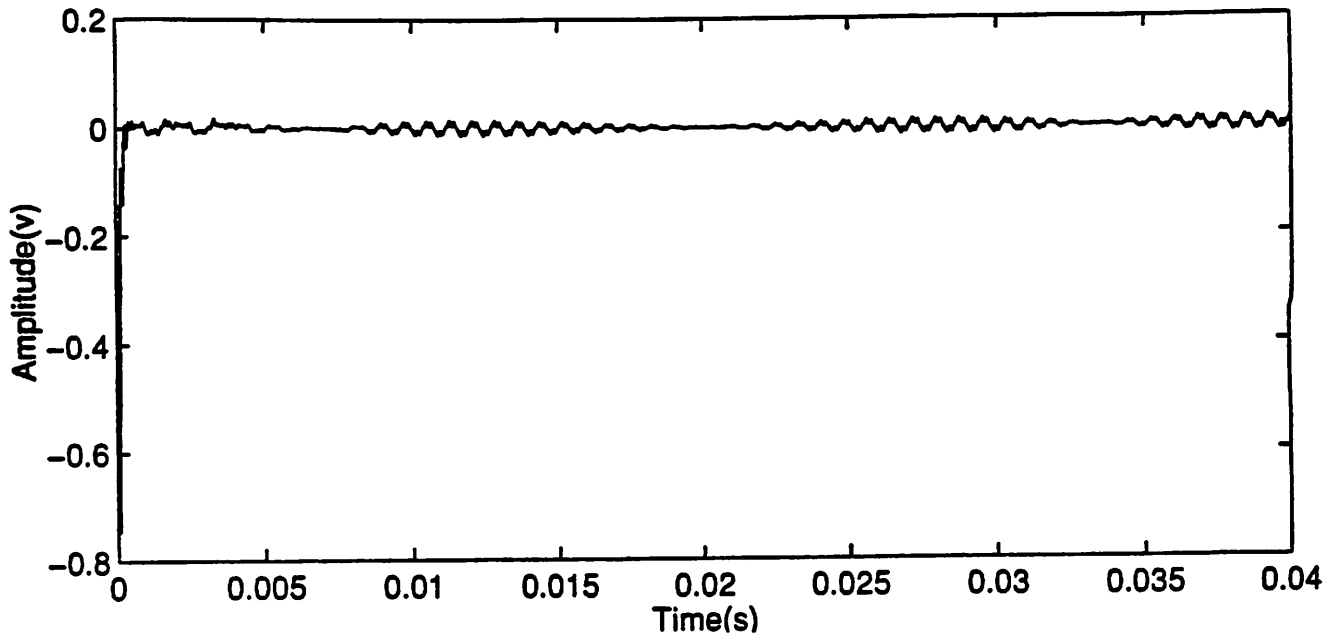


Figure 5(b)

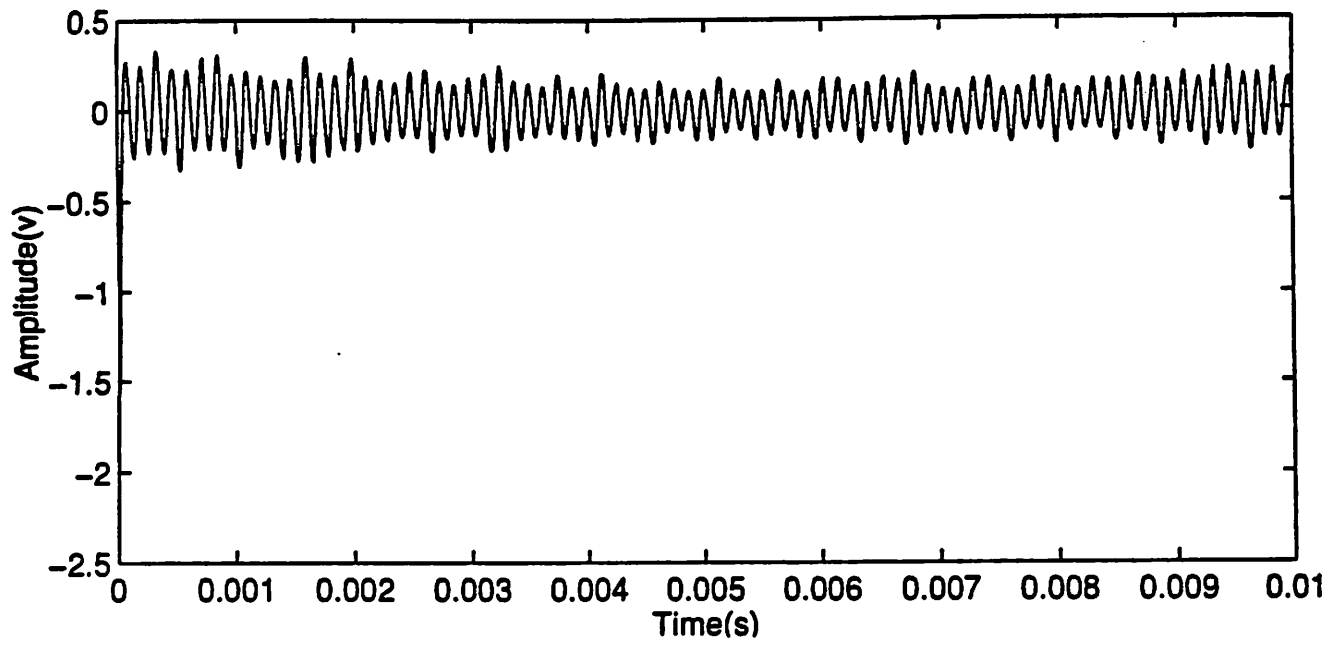


Figure 6(a)

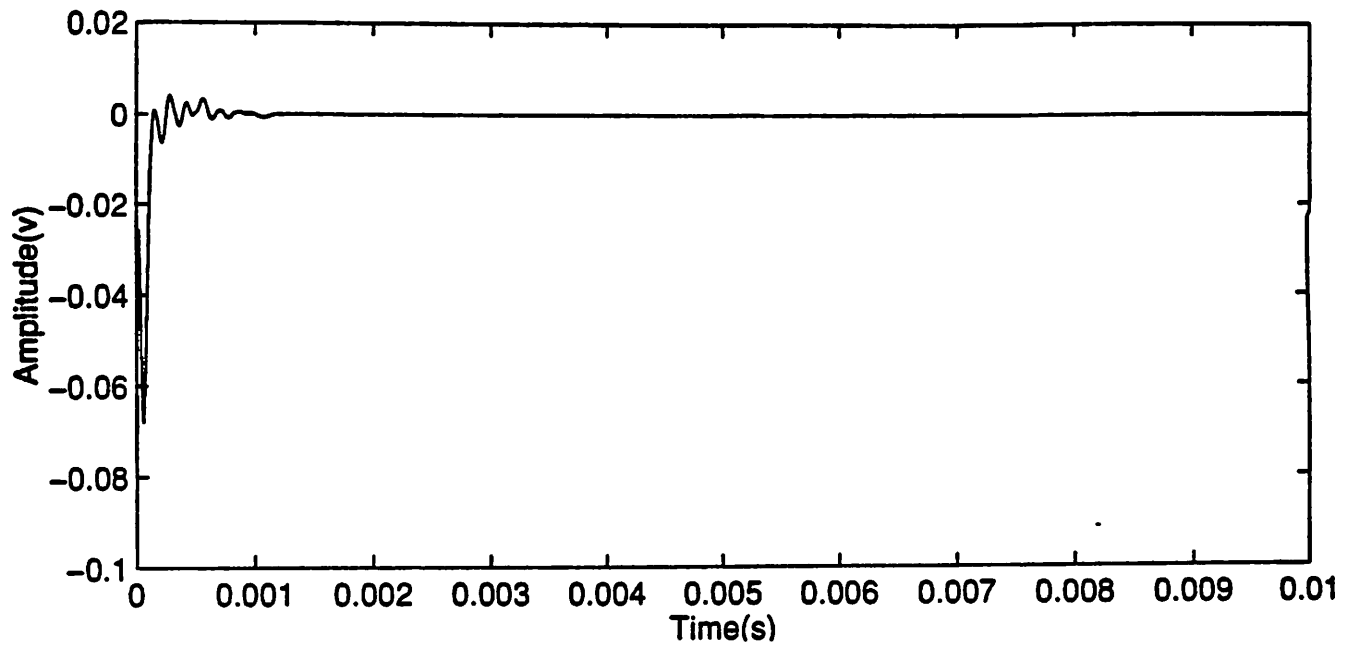


Figure 6(b)

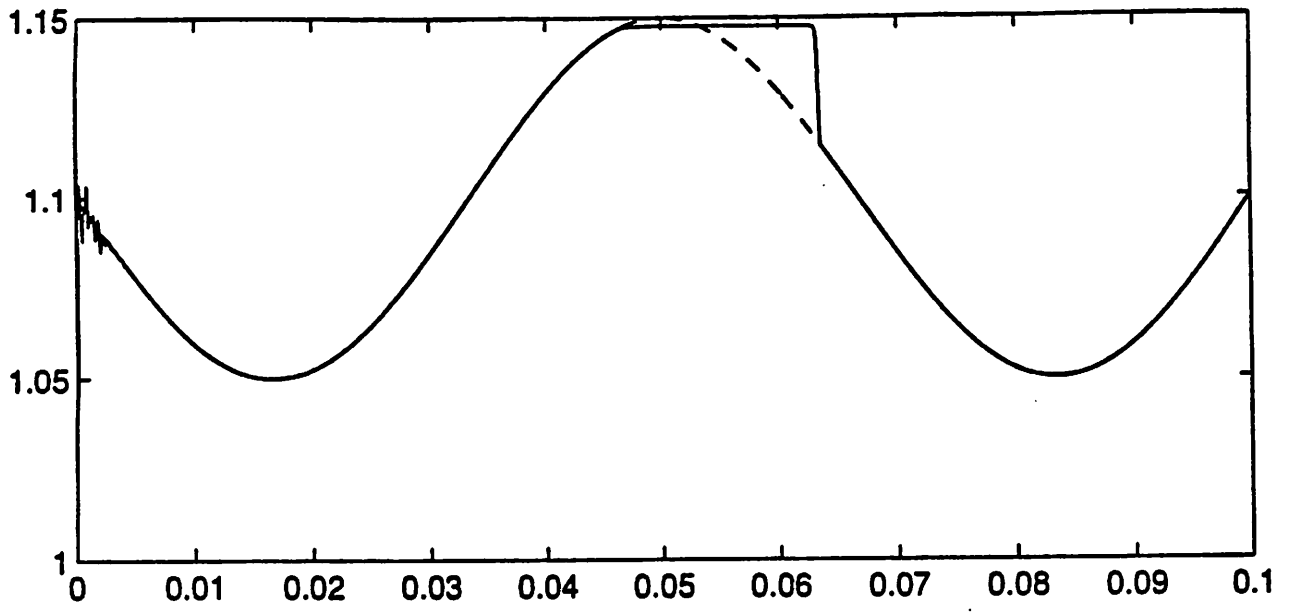


Figure 7(a)

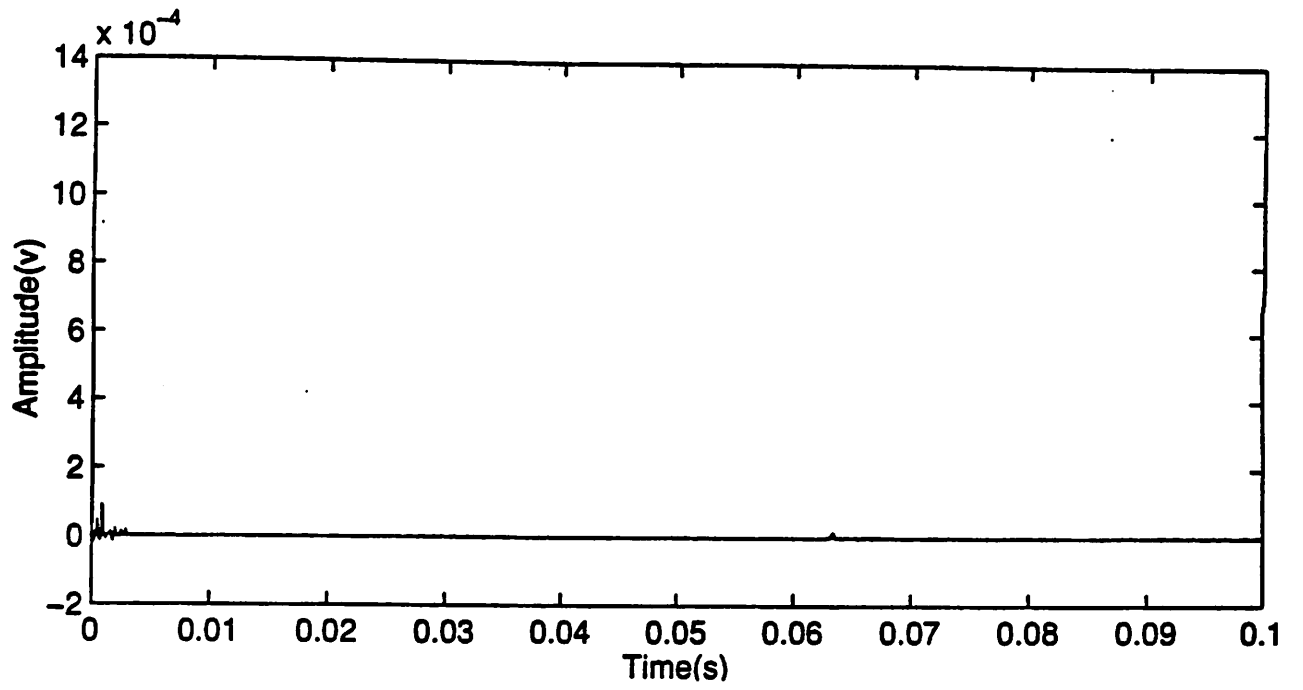


Figure 7(b)

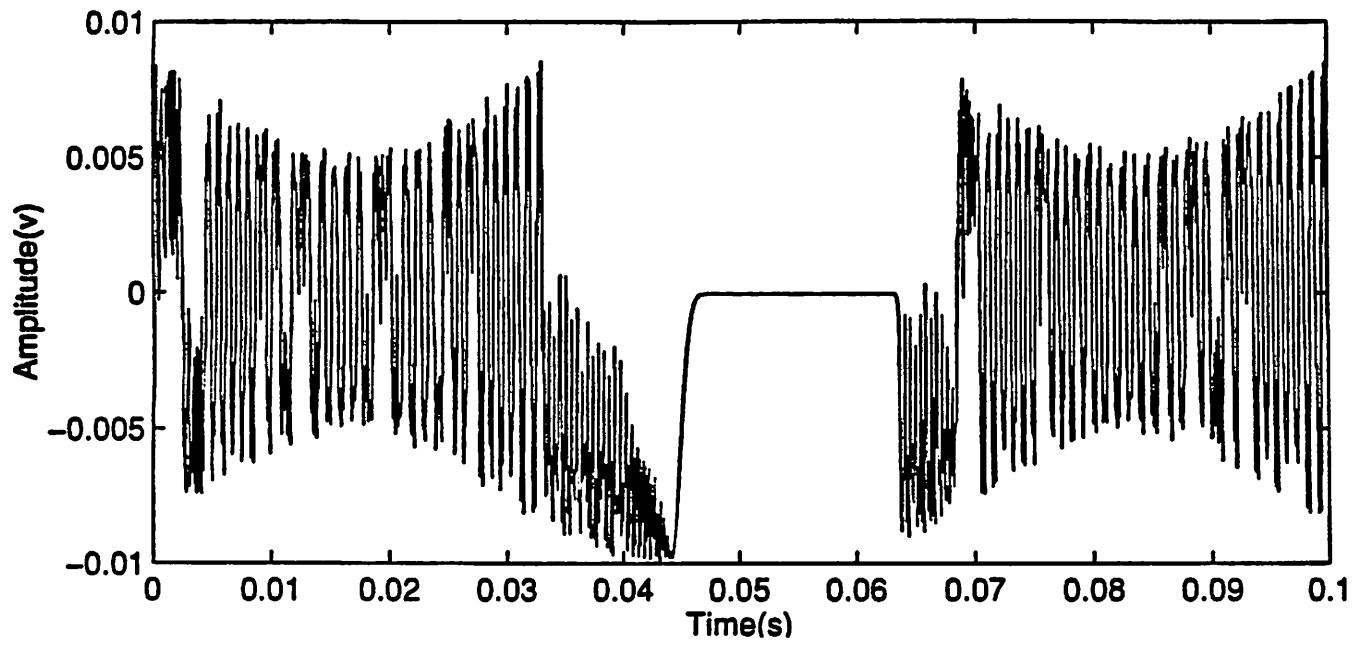


Figure 7(c)

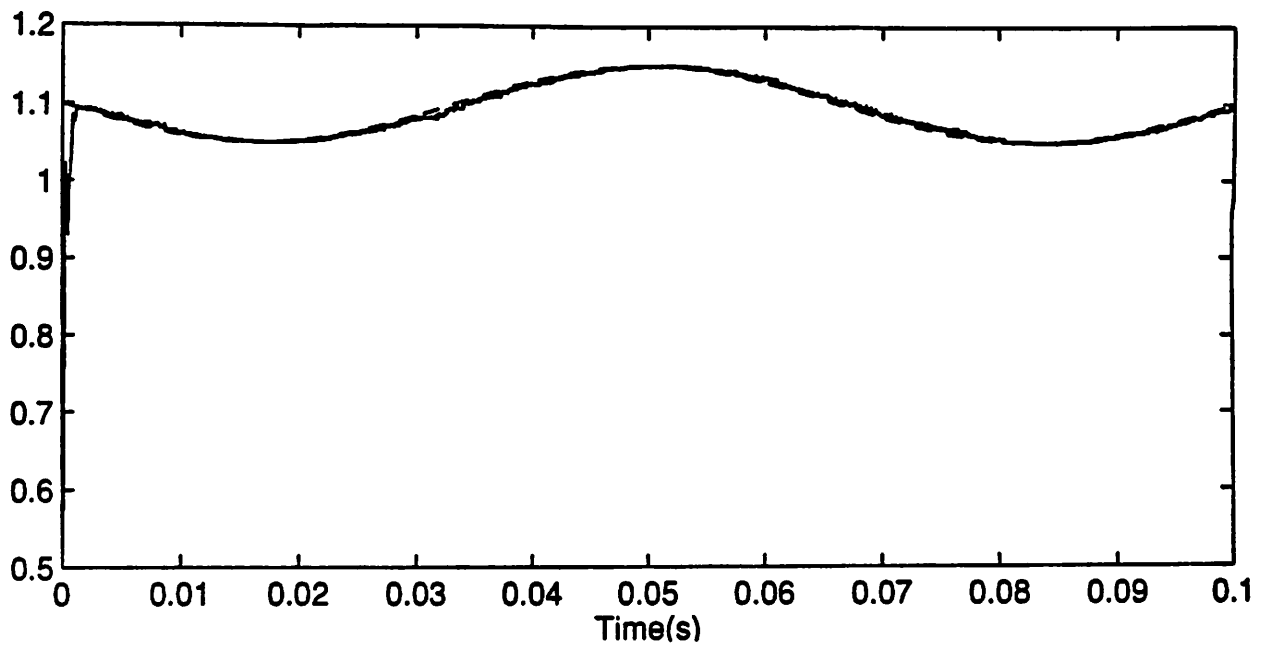


Figure 8(a)

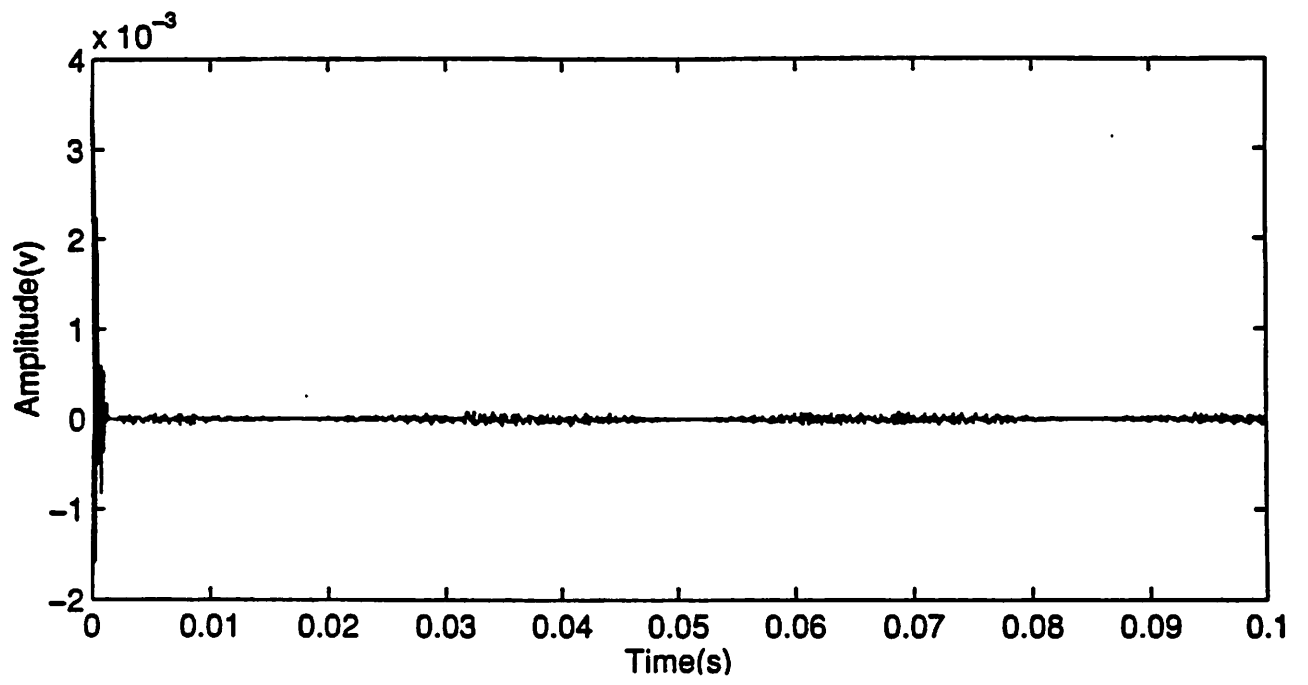


Figure 8(b)

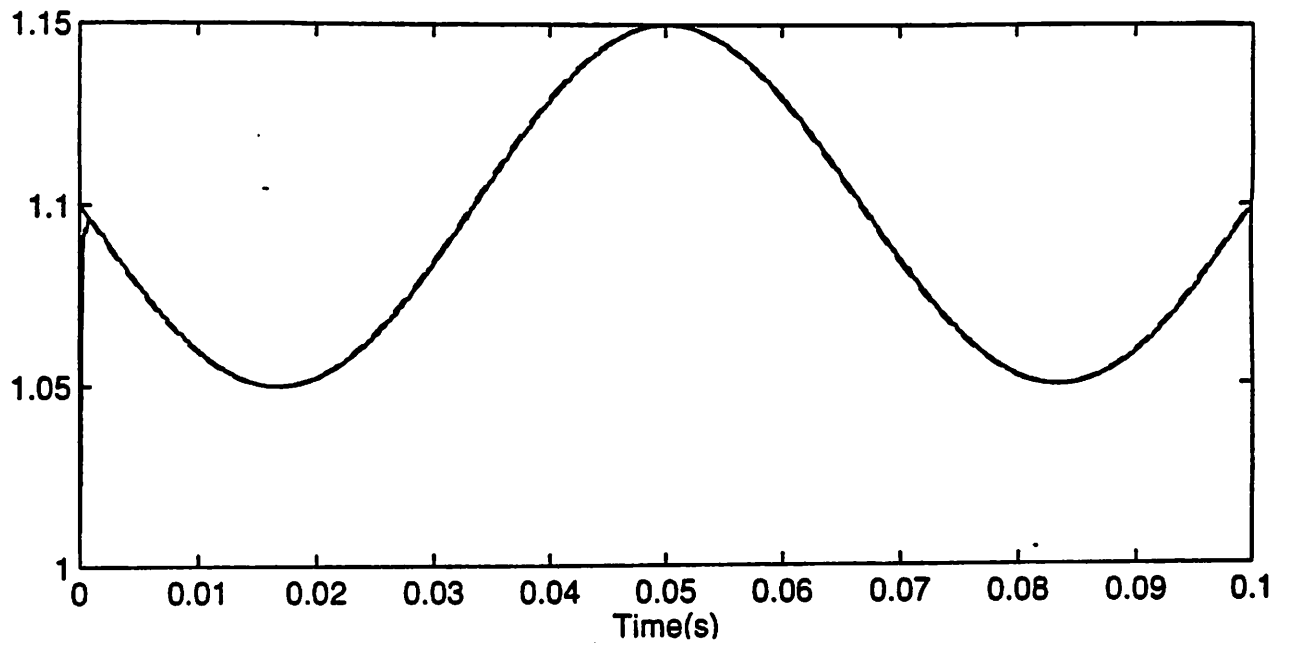


Figure 9(a)

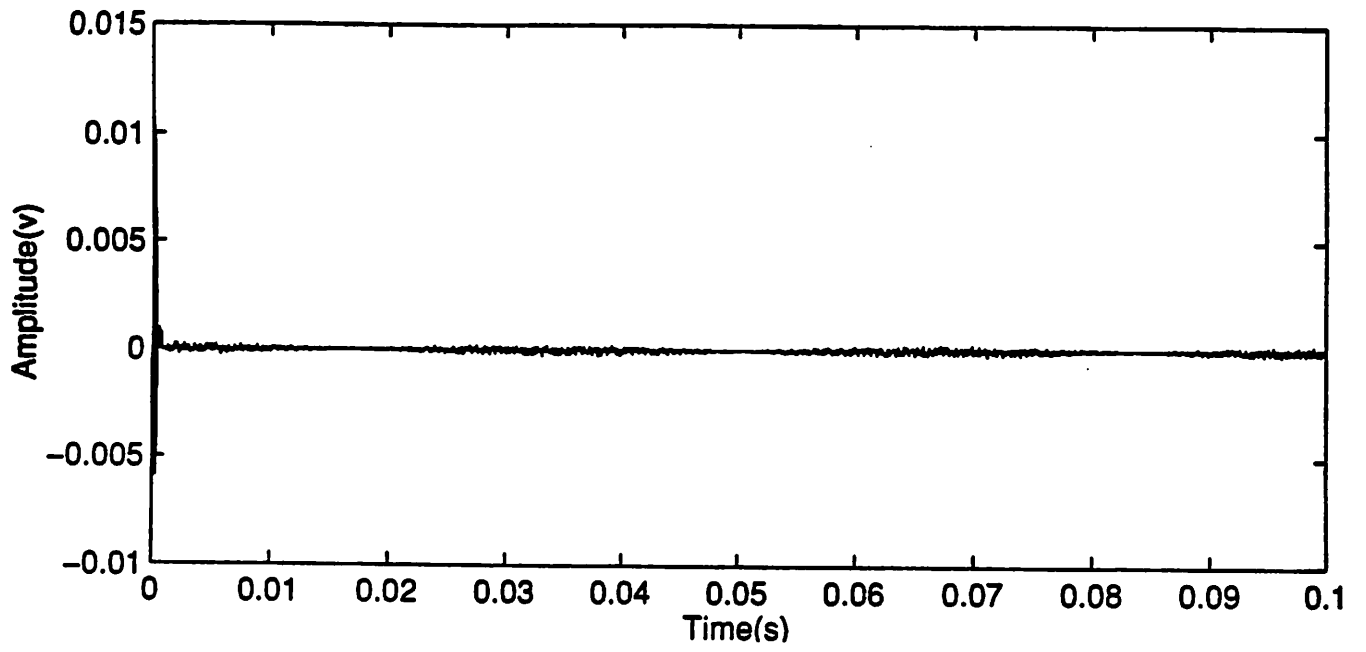


Figure 9(b)

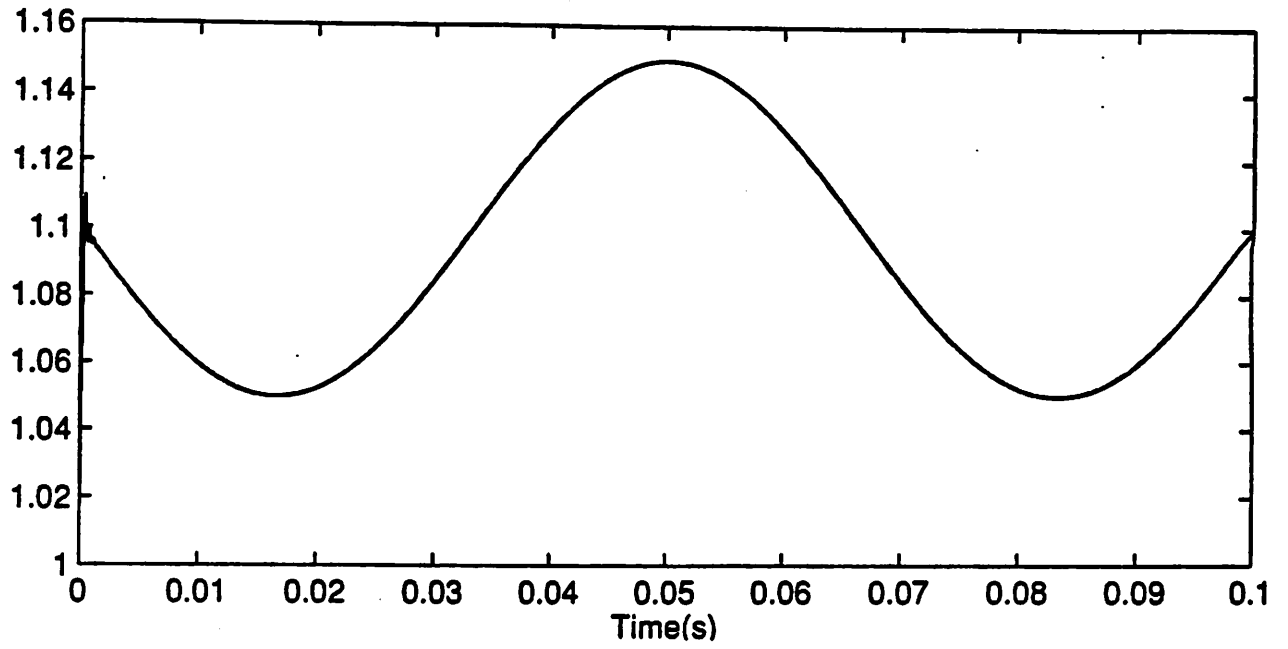


Figure 10(a)

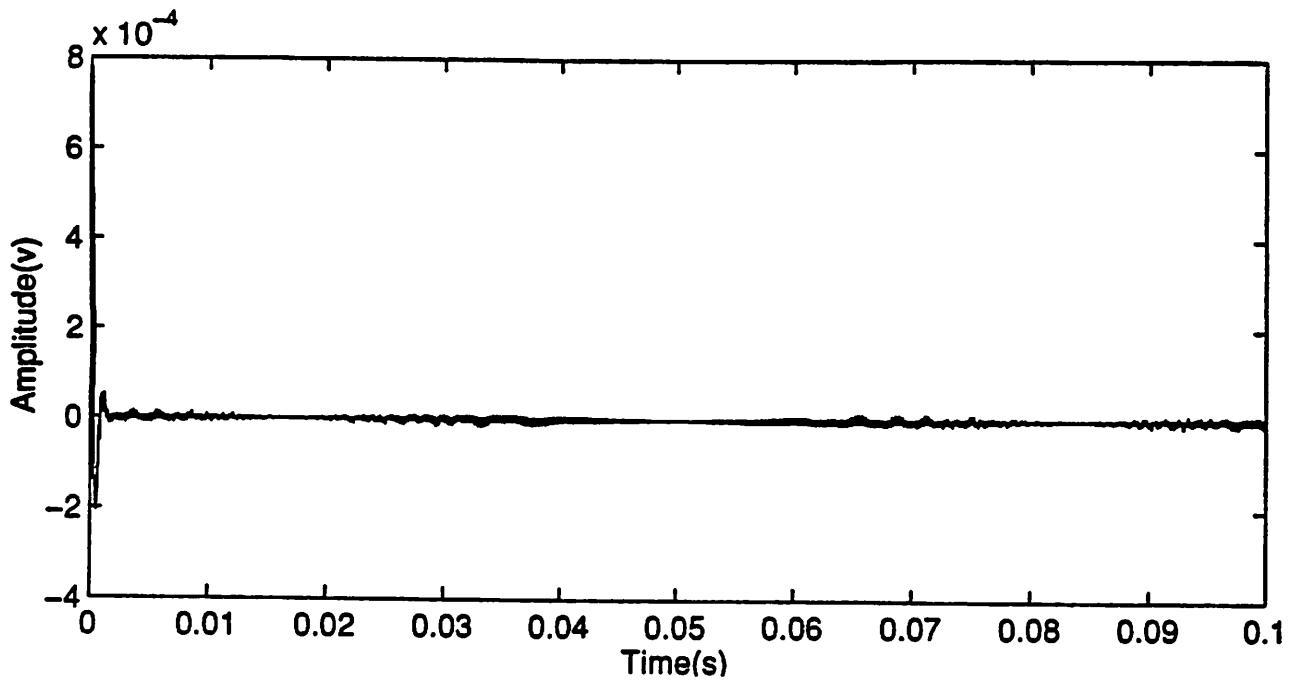


Figure 10(b)

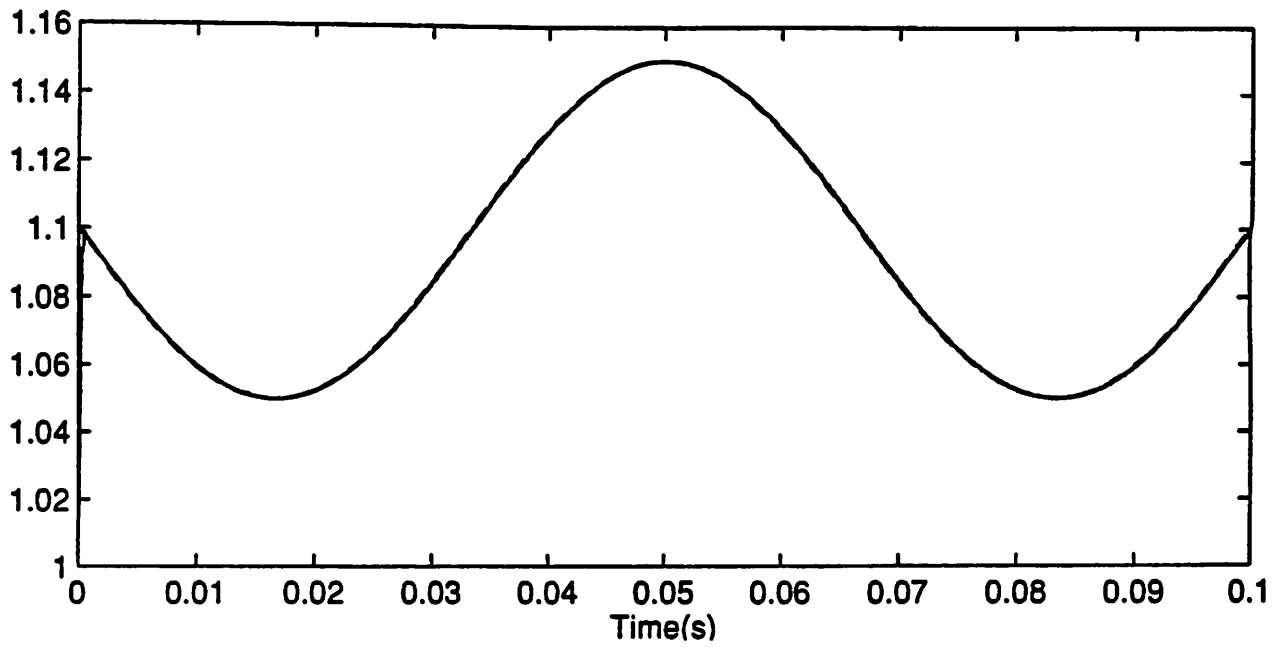


Figure 11(a)

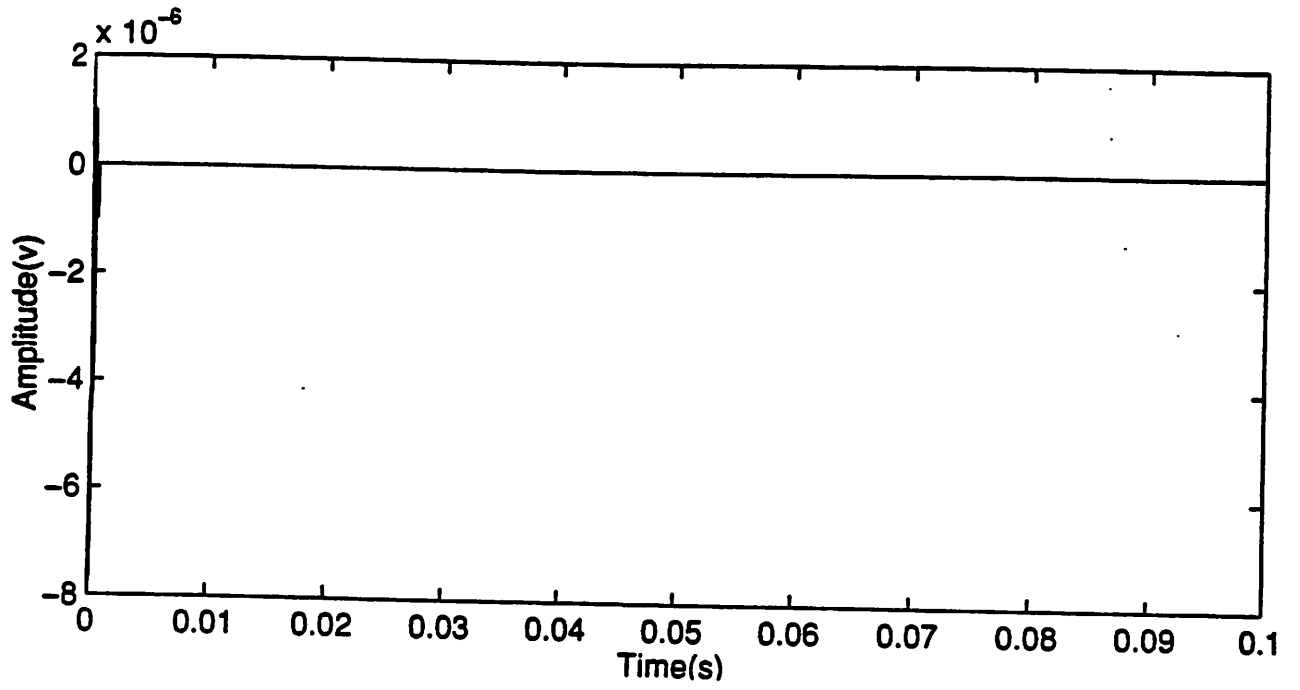
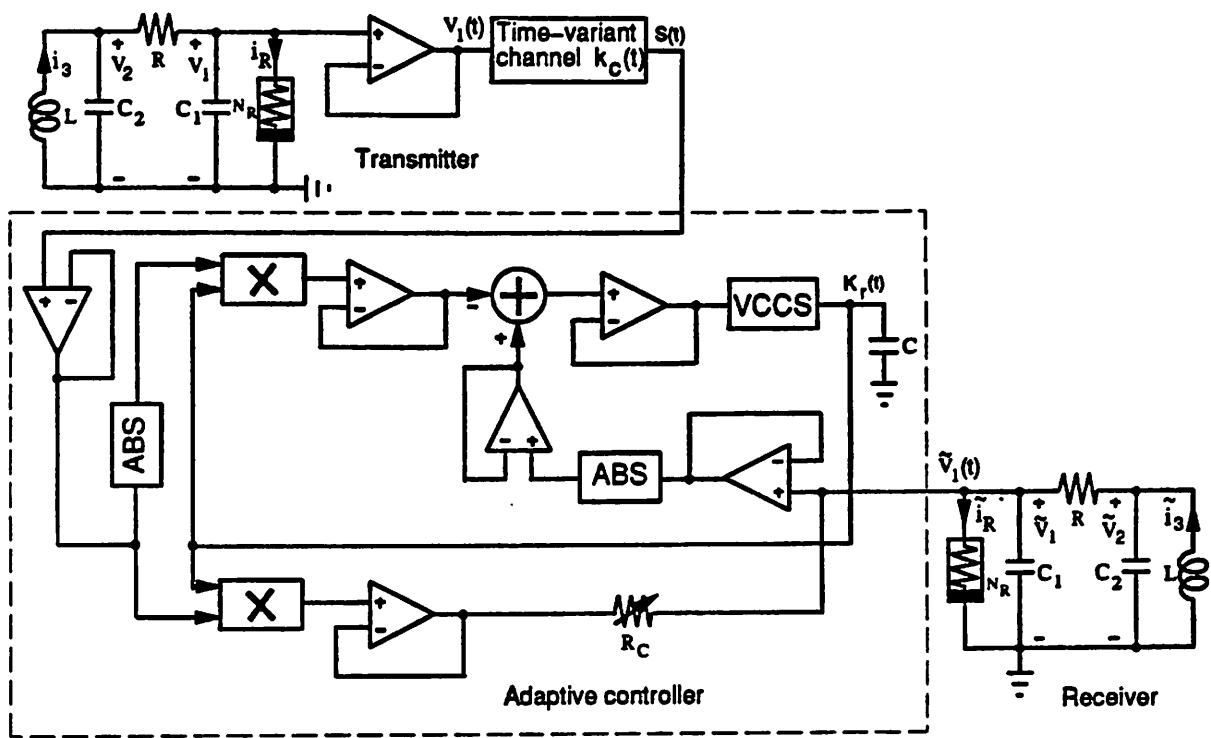
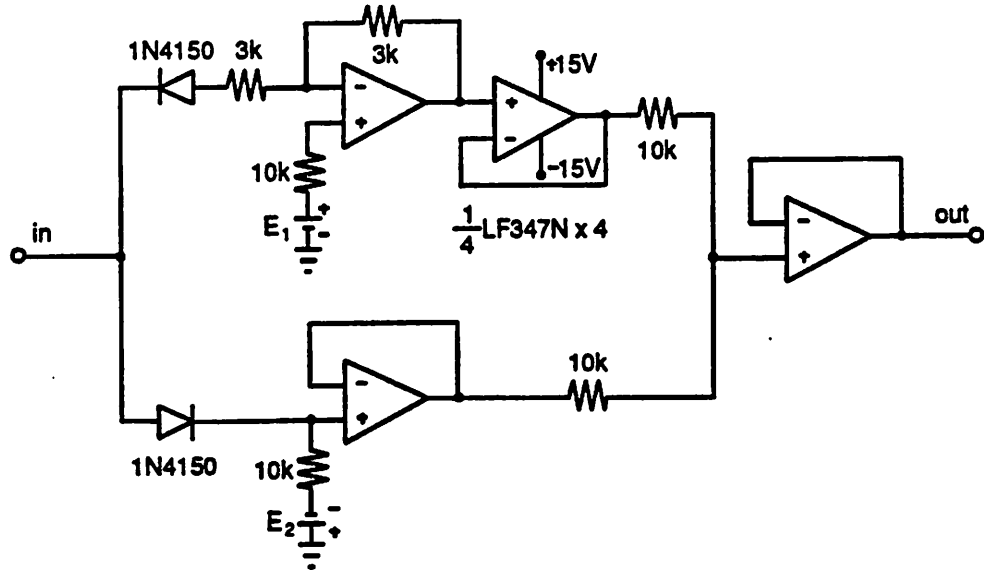


Figure 11(b)



Note: **ABS** = Absolute value function circuit shown in (b). **VCCS** = Voltage controlled current source.

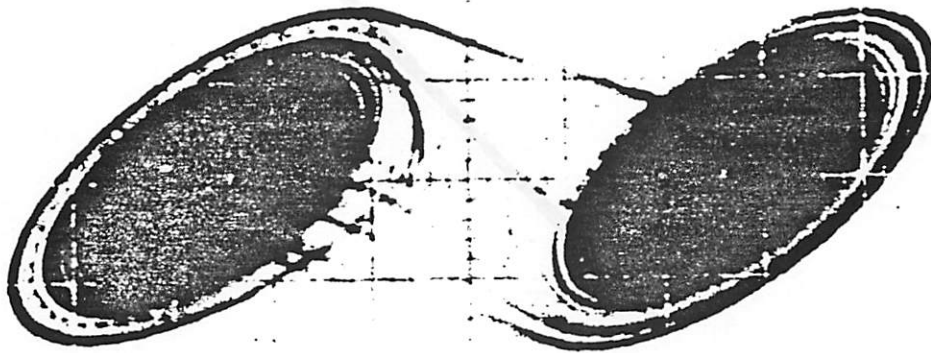
(a)



(b)

Figure 12

picln.gif



2V

1V

CH1 X

Figure 13

pic5n.gif

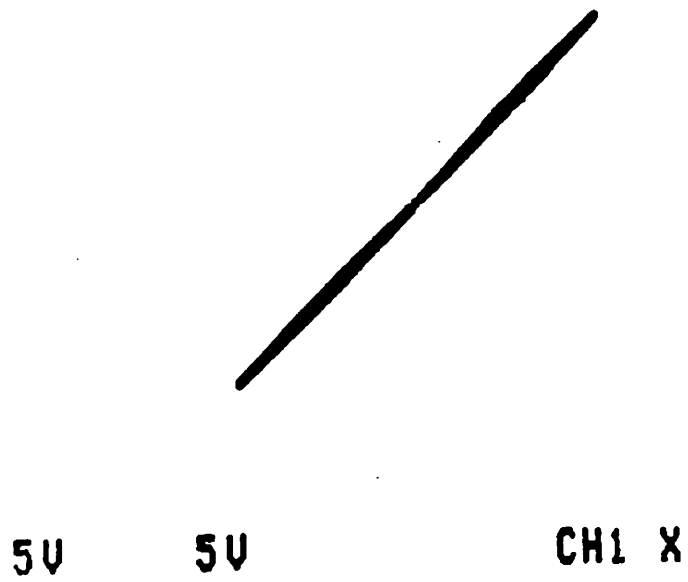


Figure 14(a)

pic7n.gif



500mV 2V

CH1 X

Figure 14(b)

pic6n.gif



5V

5V

CH1 X

Figure 15(a)

pic8n.gif

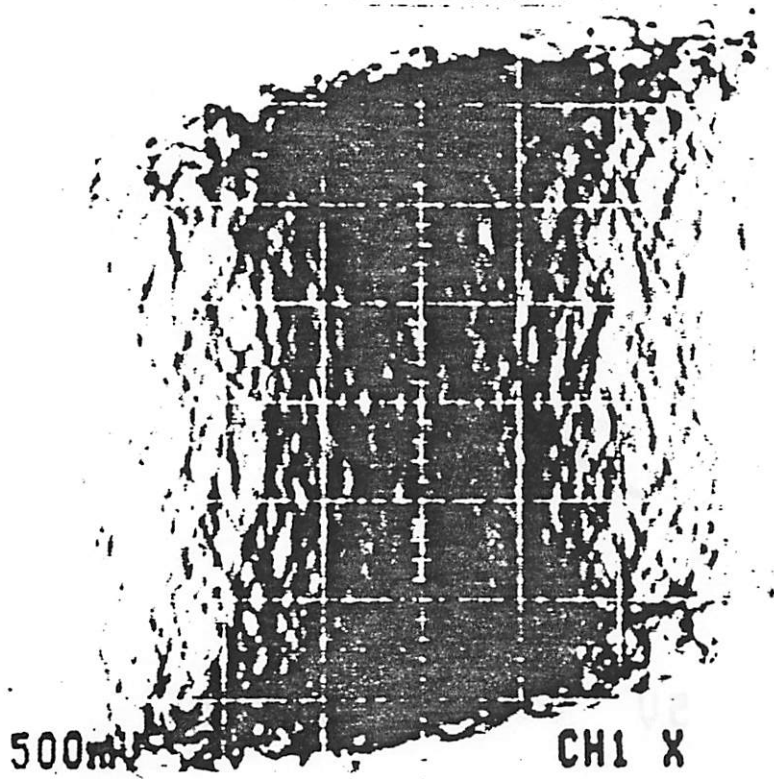
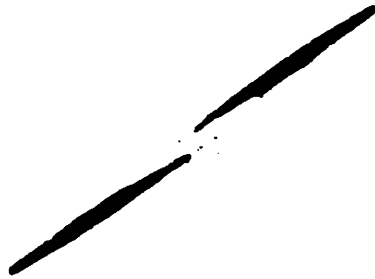


Figure 15(b)

pic9n.gif



5U

5U

CH1 X

Figure 16(a)

pic10n.gif

500mV 2V

CH1 X

Figure 16(b)

pic2n.gif

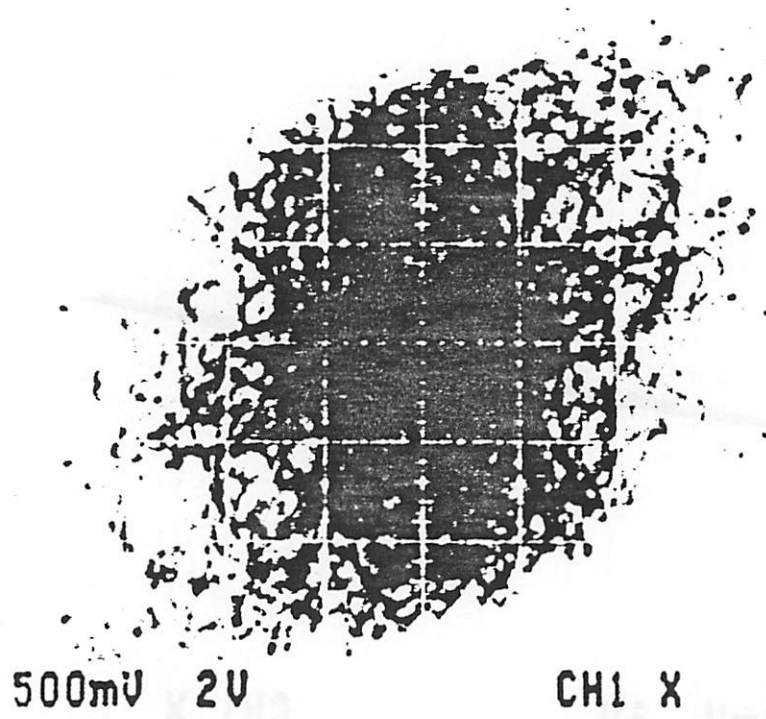


Figure 17(a)

pic3n.gif



500mV 2V

CH1 X

Figure 17(b)

pic4n.gif



500mV 2V

CH1 X

Figure 17(c)